J Electr Eng Technol Vol. 8, No. 3: 453-463, 2013
http://dx.doi.org/10.5370/JEET.2013.8.3.453

ISSN(Print) 1975-0102
ISSN(Online) 2093-7423

Impacts of Wind Power Integration on Generation Dispatch in Power Systems

Jae-Kun Lyu*, Jae-Haeng Heo†, Mun-Kyeom Kim and Jong-Keun Park***

Abstract – The probabilistic nature of renewable energy, especially wind energy, increases the needs for new forms of planning and operating with electrical power. This paper presents a novel approach for determining the short-term generation schedule for optimal operations of wind energy-integrated power systems. The proposed probabilistic security-constrained optimal power flow (P-SCOPF) considers dispatch, network, and security constraints in pre- and post-contingency states. The method considers two sources of uncertainty: power demand and wind speed. The power demand is assumed to follow a normal distribution, while the correlated wind speed is modeled by the Weibull distribution. A Monte Carlo simulation is used to choose input variables of power demand and wind speed from their probability distribution functions. Then, P-SCOPF can be applied to the input variables. This approach was tested on a modified IEEE 30-bus system with two wind farms. The results show that the proposed approach provides information on power system economics, security, and environmental parameters to enable better decision-making by system operators.

Keywords: Wind power integration, Correlated wind speed, Weibull distribution, Monte carlo simulation (MCS), Probabilistic security-constrained optimal power flow (P-SCOPF)

1. Introduction

Countries around the world are encouraging the development and integration of renewable energy sources. Sustainable and clean energy resources, especially wind power, are rapidly becoming significant generating technologies. However, the intermittency, variability, and limited predictability of wind power increase uncertainty and make power systems vulnerable. This probabilistic nature of wind creates profound challenges in planning and operating power systems, across the range from short-term regulation and balancing problems to long-term transmission network planning. Even if wind power were predicted perfectly, variability is still a vital issue that must be considered when other generation resources are being scheduled. The non-wind generation resources, namely, controllable resources, have to be dispatched skillfully considering additional safeguards for wind power integration such as sufficient reserves, demand response, and energy storage [1, 2].

Deterministic approaches have been widely used in power system planning and operation for many years. Optimal power flow (OPF) is a common tool for determining short-term generation scheduling. However, a deterministic approach may no longer represent the effects of probabilistic characteristics on dispatch results. Although probabilistic approaches to power system analysis deserve more attention in power systems that include large amounts of wind power generation, the development of such approaches is still in the early stages. Since Borkowska first proposed the probabilistic load flow in 1974 [3], some research has developed this into probabilistic optimal power flow (P-OPF). Initially, P-OPF mostly considered demand uncertainty [4-8]. However, the demand uncertainty, which is generally the only uncertainty in power system operation except for disturbances, is not very large and exhibits a periodic pattern; it can be forecast reasonably accurately based on weather and historical data. Research related to the P-OPF methodology can be classified into simulation methods and analytical methods. Simulation methods put emphasis on computational efficiency due to the large sample set involved. Analytical methods include the two-point estimate method [4-6], cumulant method [7], and first-order second-moment method [8]. The cumulant method relies on the behavior of random variables and their cumulants, and it requires calculating an inverse Hessian. The first-order second-moment method finds the statistical characteristics of random variables such as means and standard deviations. The two-point estimate method was introduced by [4] for solving P-OPF with high computational efficiency. However, the two-point estimate method may lead to inaccurate solutions when the input variables have large variances. All these approaches assume that the random variables are uncorrelated. The

† Corresponding author: School of Electrical Engineering, Seoul National University, Seoul, Korea (jhheo78@snu.ac.kr)
* School of Electrical Engineering, Seoul National University, Seoul, Korea. (handyjack@ snu.ac.kr; parkjk@snu.ac.kr)
** Department of Electrical Engineering, Dong-A University, Busan, Korea. (mkkim@dau.ac.kr)
Received: August 21, 2012; Accepted: December 4, 2012

most straightforward method of probabilistic power system analysis is by Monte Carlo simulation (MCS), which repeats a simulation with input variables selected from the probability distribution functions (PDFs) of random variables. It is often used for its accurate solutions and simple implementation, in spite of the large computational effort required. Above all, a MCS makes using existing deterministic OPF for the inputs possible.

Since security is the most crucial aspect of a system operator's planning and operation of a power system, security tools and practices are commonly used, such as security-constrained unit commitment (SC-UC) or security-constrained optimal power flow (SCOPF) [9-12]. Since the security problem becomes more critical due to larger uncertainties in wind energy-integrated power systems, the existing P-OPF has to be developed to involve security constraints, such as limits for the transmission line flow and bus voltage. The security issues, however, have been a much-neglected branch of P-OPF research until now. Furthermore, most research dealing with wind power integration has assumed a single wind turbine or wind farm, not considering the circumstances of the wind power boom. With large numbers of wind turbines in multiple wind farms, correlated wind speed modeling is useful for predicting the aggregate wind power generation, regardless of wind speed forecasting techniques [13, 14]. This method also facilitates studies on the impact of future wind farm installations. To generate realistic and synthetic random variables of wind speeds at different locations, correlated wind speeds have been used for proposed probabilistic security-constrained optimal power flow (P-SCOPF). Cholesky decomposition [15], which is the most common technique for generating multivariate distributions of random variables, was used to obtain the correlated wind speeds with efficient computation. Although the Cholesky decomposition allows only the simulation of a single operating point, it amounts to nothing for P-SCOPF, which handles generation scheduling.

In this paper, we considered the limits of transmission flow and bus voltage in pre- and post-contingency cases as security constraints. We also applied correlated wind speeds generated by the Weibull distribution function to a proposed P-SCOPF methodology. The proposed method provides information on power system security, economics, and environmental aspects to system operators so that they can make better decisions for power system operation.

Therefore, in this work, the P-SCOPF problem includes the following:

- uncertainty modeling for demand and wind speed;
- MCS for choosing input variables of demand and wind speed;
- network constraints (AC power flow equations); and
- security constraints (transmission flow limits in pre- and post-contingency cases).

The remainder of this paper is organized as follows. Section 2 deals with modeling uncertainties for the P-SCOPF problem. Section 3 describes the correlated wind speed and power in detail. Section 4 presents the mathematical formulation of P-SCOPF with its solution procedure, while Section 5 presents and discusses numerical results. Section 6 summarizes our conclusions.

2. Uncertainty Modeling

2.1 Normal distribution for demand uncertainty

The system demand has a periodic pattern that changes based on many factors such as temperature and day of the week. The variability of demand is smaller than that of wind speed and the forecasting is fairly accurate, especially in the short term. Generally, demand uncertainty for short-term scheduling can be modeled as a normal distribution [16], which is expressed as follows:

$$\mathrm{f}_{\mathrm{P_D}}(p_D) = \frac{1}{\sigma_D\sqrt{2\pi}}\,\mathrm{e}^{-\frac{(\mathrm{p_D}-\mu_D)^2}{2\sigma_D^2}} \tag{1}$$

2.2 Weibull distribution for wind uncertainty

The wind speed cannot be described by a normal distribution due to its high variability and intermittency. International Electrotechnical Commission (IEC) standards recommend modeling wind speed at a certain location using a two-parameter Weibull or Rayleigh distribution. The Weibull distribution is one of the most commonly used distributions in various fields due to its flexibility, and it is appropriate for reflecting wind speed. The Weibull distribution can have various distribution forms, depending on the value of its shape parameter k. The Rayleigh distribution is a specific Weibull distribution form where the shape factor $k = 2$. The general structure of the two-parameter Weibull PDF is written as shown in these equations:

$$f(v) = \begin{cases} 0 & v < 0 \\ \frac{k}{c}\left(\frac{v}{c}\right)^{k-1} e^{-\left(\frac{v}{c}\right)^k} & v \geq 0 \end{cases} \tag{2}$$

$$\mu_V = c\Gamma\left(1+\frac{1}{k}\right) \tag{3}$$

$$\sigma_V^2 = c^2\left[\Gamma\left(1+\frac{2}{k}\right) - \Gamma^2\left(1+\frac{1}{k}\right)\right] \tag{4}$$

3. Correlated Wind Speed and its Power

3.1 Wind speed correlation

Generally, the consideration of correlation between wind speeds has great influence on electrical networks with wind

farms. Given series of wind speeds at different locations, a correlation coefficient can be calculated from the covariance and standard deviations of the wind speeds at each location. Here, the correlation coefficient represents the degree of relationship among the series of wind speeds. The correlation coefficient is defined in the following equation:

$$\rho = \frac{\sigma_{12}^2}{\sigma_1 \cdot \sigma_2} \tag{5}$$

where ρ is the correlation coefficient, $\sigma_{1,2}$ is the covariance between series 1 and 2, and σ_1 and σ_2 are the standard deviations of both series.

A close relationship exists between the distance among the wind farms and the correlation of their wind speeds due to similar meteorological conditions [17]. The locations far from each other have a small correlation close to 0 or even a negative correlation, while locations in close proximity have a positive correlation close to 1, or at least greater than 0.8. Thus, we assume that correlation of wind speed in the same wind farm is sufficiently highly correlated, i.e., correlation is greater than 0.8. Therefore, we obtain the generated power of a wind farm using this equation:

$$P_{WF} = N_{WT,n} \cdot P_{WT} \tag{6}$$

On the other hand, due to the weak correlation of wind speeds in widely separated wind farms, wind speeds at each location should be necessary. The mean and standard deviation of the wind speeds at the locations can easily be calculated and they are used to generate Weibull random variable vectors. However, these vectors are independent of each other yet. To make the wind speeds vary as a correlated set, it requires producing a joint Weibull distribution which consists of multivariate random variable vectors. The multivariate Weibull random variable vectors are obtained by following procedure.

Step 1. Find the mean value and standard deviation based on the hourly historical wind speeds during a year for each location. The scale parameter c and shape parameter k of the Weibull distribution vary depending on the geographical condition of a location. Several sources provide guidance in determining these two parameters from wind speed data [18,19]. In this paper, we easily implemented this Weibull distribution using MATLAB; it provides the *wblfit*() function, which returns the maximum likelihood estimates of the parameters of the Weibull distribution given the wind speeds vectors.

Step 2. Find the correlation coefficient ρ of wind speeds at these locations using the MATLAB *corr*() function, which returns a matrix containing the pairwise linear correlation coefficient.

Step 3. Produce an uncorrelated random variable vector $\boldsymbol{z}$ that consists of univariate random variables with mean value μ_z and correlation matrix Ω_z using the Step 1 results for scale parameter c and shape parameter k. The z_1 indicates the Weibull distribution of wind farm 1 only. This can be implemented using the MATLAB function *wblrnd*(), which returns an array of random numbers chosen from the Weibull distribution with c and k. Then, the uncorrelated vector $\boldsymbol{z}$ is expressed as shown in the following equations:

$$\boldsymbol{z} = (z_1, z_2, \dots, z_n)^{\mathrm{T}} \tag{7}$$

$$\boldsymbol{z} = (z_1, z_2, \dots, z_n)^{\mathrm{T}} \tag{8}$$

$$\boldsymbol{z} = (z_1, z_2, \dots, z_n)^{\mathrm{T}} \tag{9}$$

Here, we need to introduce a new vector y to obtain the joint Weibull distribution, which consists of multivariate random variables $y_1, y_2, \dots, y_n$. The correlated and uncorrelated random variable vectors $\boldsymbol{y}$ and $\boldsymbol{z}$ have following relationship according to the Cholesky decomposition method, which consists of a lower triangular matrix L and its transposition one L^T.

$$\boldsymbol{y} = L \cdot (\boldsymbol{z} - \mu_z) + \mu_y \tag{10}$$

$$\Omega_y = L \cdot L^T \tag{11}$$

Step 4. Use the MCS method to select correlated wind speeds v randomly from Weibull distribution $\boldsymbol{y}$. Equation (10) denotes that if a wind speed for wind farm y_1 is obtained, wind speeds for the other wind farms $y_2, \dots, y_n$ are determined automatically using a Cholesky matrix that connotes their correlation. For chosen inputs of wind speeds, the deterministic approach can easily be applied for system analysis.

3.2 PDF for generated power of a wind turbine

The active power output generated from a wind turbine can be represented as a function of the wind speed $\boldsymbol{V}$. The most frequently used quadratic model for expressing wind turbine power is described by

$$P_w(v) = \begin{cases} 0 & v < v_{in} \\ P_R \dfrac{v^2 - v_{in}^2}{v_r^2 - v_{in}^2} & v_{in} < v < v_r \\ P_R & v_r < v < v_{out} \\ 0 & v > v_{out} \end{cases} \tag{12}$$

Fig. 1 shows the quadratic power curve for a Vestas V100 wind turbine, which is used for the numerical example in Section 5. The PDF for the generated power of a wind turbine is a function of wind power P_W. Each part of

the power curve in Eq. (12) should be analyzed separately on the PDF for generated power of a wind turbine depending on the value of v_{in}, v_r, and v_{out}. Hence, the PDF for generated power can be divided and expressed as follows [16].

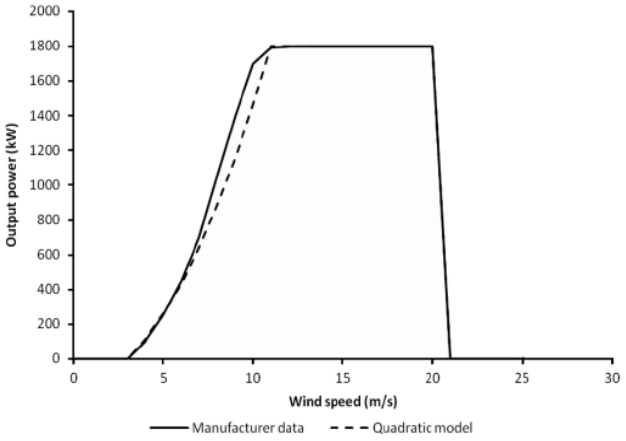

Fig. 1. Power curve for the Vestas 1.8 MW wind turbine.

$$f_P[P_w(v)] = \begin{cases} 0 & P_w < 0, P_w > P_R \\ \left(1 + e^{-\left(\frac{v_{out}}{c}\right)^k} - e^{-\left(\frac{v_{in}}{c}\right)^k}\right)\delta(P_w) & P_w = 0 \\ \frac{k'}{c'}\left(\frac{P_w - \gamma'}{c'}\right)^{k'-1} e^{-\left(\frac{P_w-\gamma'}{c'}\right)^{k'}} & 0 < P_w < P_R \\ \left(e^{-\left(\frac{v_r}{c}\right)^k} - e^{-\left(\frac{v_{out}}{c}\right)^k}\right)\delta(P_w - P_R) & P_w = P_R \end{cases}$$
$$c' = P_R \frac{v^2}{v_r^2 - v_{in}^2} \qquad k' = \frac{k}{2} \qquad \gamma' = -P_R \frac{v_{in}^2}{v_r^2 - v_{in}^2} \tag{13}$$

Finally, the aggregate wind power is

$$f_P\left(P_{w,total}\right) = \sum_{n=1}^{N_{WF}} N_{WT,n} \cdot f_P\left[P_w(v)_{n,m}\right] \tag{14}$$

4. Problem Formulation

4.1 P-SCOPF

The input variables of system demand and wind speed are randomly selected from their PDF by MCS. Then, the deterministic SCOPF is used to analyze the system state for the selected input variables. The SCOPF is formulated as a nonlinear optimization problem, as shown in (15). In the objective function of SCOPF, quadratic cost function for operating cost, which is the most common model for operation tools such as ED and OPF, has been used. As SCOPF is a tool for short-term generation scheduling, maintenance and investment cost are not considered in this study. The wind generation of bus i should be subtracted from the demand of that bus as we utilized PQ bus modeling (negative demand) for the wind turbine. In addition, the transmission network loss P_L is considered in the problem, since power plants are spread out geographically.

$$min \sum_{i=1}^{NG} \left(a_i P_i^2 + b_i P_i + c_i\right) \tag{15}$$

subject to the following constraints:

1. power demand balance

$$P_{G_i}(\boldsymbol{V}, \boldsymbol{\delta}) = P_{G_i} - P_{D_i} - P_w = \sum_{j=1}^{NG} |V_i||V_j| \left[G_{ij} cos\left(\theta_i - \theta_j\right) + B_{ij} sin\left(\theta_i - \theta_j\right)\right] \tag{16}$$

$$Q_i(\boldsymbol{V}, \boldsymbol{\delta}) = Q_{Gi} - Q_{Di} = \sum_{j=1}^{NG} |V_i||V_j| \left[G_{ij} sin\left(\theta_i - \theta_j\right) - B_{ij} cos\left(\theta_i - \theta_j\right)\right] \tag{17}$$

2. power output limit of conventional generating units

$$P_i^{min} \le P_i \le P_i^{max} \tag{18}$$

$$Q_i^{min} \le Q_i \le Q_i^{max} \tag{19}$$

3. power output limit of wind turbines

$$0 \le P_w(v)_{n,m} \le P_R \tag{20}$$

4. bus voltage limit

$$V_i^{min} \le V_i \le V_i^{max} \tag{21}$$

5. steady-state transmission flow limits of line l

$$-PL_l^{max} \le PL_l = \sum_{i=1}^{M} A_{l,i}\left[P_i + P_{\emptyset,i} - \left(P_{D,i} - P_w(v)_{n,m}\right)\right] \le PL_l^{max} \tag{22}$$

6. contingency state transmission flow limits of line l

$$-PL_l^{max} \le PL_l = \sum_{i=1}^{M} E_{l,i}(j)\left[P_i + P_{\emptyset,i} - \left(P_{D,i} - P_w(v)_{n,m}\right)\right] \le PL_l^{max} \qquad j = 1,2,\dots,N_C \tag{23}$$

Linear sensitivity factors are used to formulate transmission flow limits in pre- and post-contingency conditions.

Fossil fuel-fired thermal generating units decrease their power output equivalent to the amount generated by wind. This leads to a commensurate expected reduction in operating cost and CO_2 emissions. Even though reducing CO_2 emissions is not a primary target of this paper, this comes as a by-product of using a clean energy source like wind. The amount of CO_2 emissions produced when unit i generates at power level P_i is expressed as

$$E_i(P_i) = \alpha_i P_i^2 + \beta_i P_i + \gamma_i + \zeta_i \exp(\lambda_i P_i) \qquad (24)$$

4.2 Solution procedure

The proposed approach is implemented sequentially, as shown in Fig. 2.

***Step* 1**: Start the initial configuration with available system information.

Step 2: Produce the PDF of the demand according to a normal distribution.

Step 3: Use Eqs. (2) - (4) to find the mean μ, standard deviation σ, scale parameter c, and shape parameter k. Determine the Weibull distribution model to produce correlated wind speeds using the procedures described in Section 2.2.

***Step* 4**: This gives PDFs of two uncertainties: demand and wind speeds. Randomly select inputs from the probability distributions of random variables using MCS. Then, for every selected input, use the deterministic optimal power flow to determine the optimal solution.

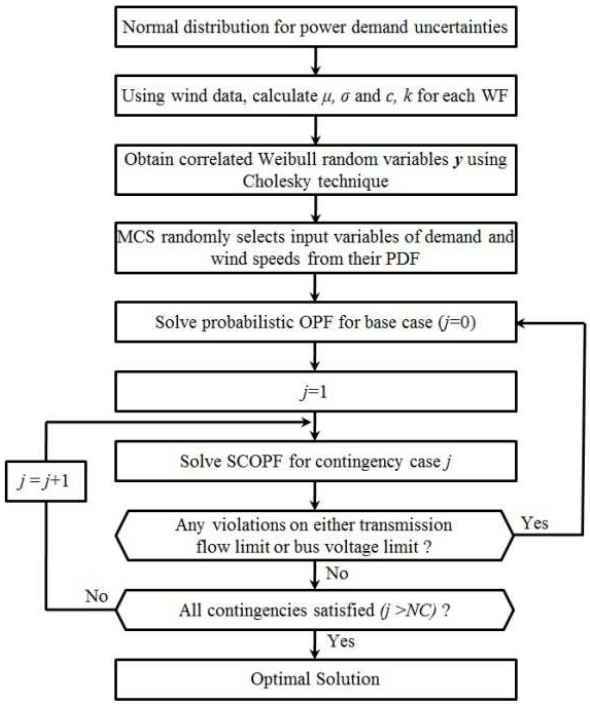

Fig. 2. Flowchart of the P-SCOPF procedure.

Step 5: Solve SCOPF for contingency case j until all contingencies are satisfied to account for the transmission line security constraint.

Step 6: Repeat these processes until no violations on either transmission flow limit or bus voltage limit are found.

5. Case Study

The validity of the proposed method was tested on a modified IEEE 30-bus system with eight generating units (six conventional units and two wind farms), 41 transmission lines, and 20 demand sides. Fig. 3 shows a single-line diagram of the test system; the other data related to the test system can be found in [20]. Table 1 gives the mean value of demand for each bus, which is

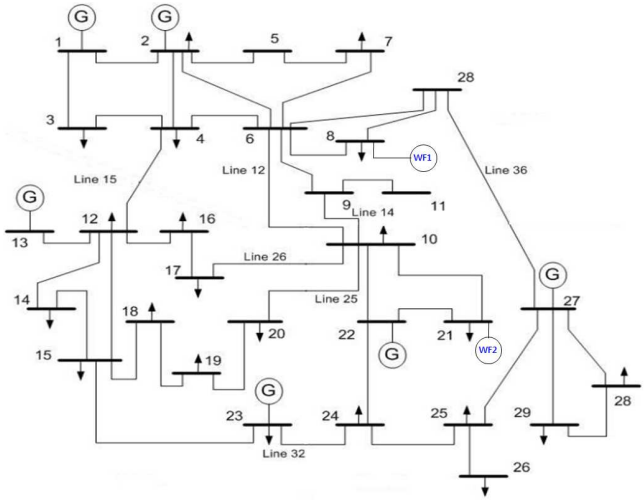

Fig. 3. Modified IEEE 30-bus system with 2 wind farms.

Table 1. Mean value of power demand.

Bus	Mean active demand [MW]	Mean reactive demand [MVar]	Standard deviation [MW]
2	21.7	21.7	1.085
3	2.4	1.2	0.12
4	7.6	1.6	0.38
7	22.8	10.9	1.14
8	30	30	1.5
10	5.8	2	0.29
12	11.2	7.5	0.56
14	6.2	1.6	0.31
15	8.2	2.5	0.41
16	3.5	1.8	0.175
17	9	5.8	0.45
18	3.2	0.9	0.16
19	9.5	3.4	0.475
20	2.2	0.7	0.11
21	17.5	11.2	0.875
23	3.2	1.6	0.16
24	8.7	6.7	0.435
26	3.5	2.3	0.175
29	2.4	0.9	0.12
30	10.6	1.9	0.53

considered to follow a normal distribution with a standard deviation of 5%. Table 2 shows the cost and emission coefficient data for the thermal generating units. We assumed that wind power generation is emission-free and consumes no fuel.

Two wind farms, WF1 and WF2, inject power directly into the transmission system at buses 8 and 21, respectively. Each wind farm contains 20 Vestas V100 1.8-MW wind turbines, with a total capacity of 36 MW. The total wind power capacity of 72 MW is thus approximately 20% of the total generation capacity. Many countries target a 20% penetration of wind power by the year 2030. The proposed approach consists of two parts: MCS for selecting the demand and wind speed input variables, and SCOPF. A standard Pentium PC with a 3.0-GHz processor and 2 GB of random access memory was used to test the proposed model with Primal-dual interior point method [21, 22].

Table 2. Cost and emission coefficient data for thermal generating units.

Bus	Fuel cost coefficient			CO2 emission coefficient				
	a	*b*	*c*	*α*	*β*	*γ*	*ζ*	*λ*
1 (G1)	0.02	2	0	0.0126	-1.1	22.983	2.0e-4	0
2 (G2)	0.0175	1.75	0	0.0200	-0.1	25.313	5.0e-4	0
13 (G3)	0.025	3	0	0.0270	-0.01	25.505	1.0e-6	0
22 (G4)	0.0625	1	0	0.0291	-0.005	24.900	2.0e-3	0
23 (G5)	0.025	3	0	0.0290	-0.004	24.700	1.0e-6	0
27 (G6)	0.00834	3.25	0	0.0271	-0.0055	25.300	1.0e-5	0

5.1. Power demand uncertainty

In general, sufficient samples for MCS ensure accurate, reliable results. To determine a reasonable sample size for the MCS, the relationship between the sample size and its performance is examined. Table 3 shows the mean value and standard deviation of operating cost and computation time for 20 implementations with different numbers of samples. The error rate of the standard deviation, which indicates the simulation fallibleness, is defined as follows:

$$\varepsilon_\sigma = \frac{100 \cdot \sigma_{No.samples}}{\mu_{No.samples}} \tag{25}$$

The computation time increases in almost direct proportion to the number of MCS samples while the error rate of standard deviation decreases. In particular, it is interesting to note that the error rate has decreased considerably in case of 1,000 samples. From the results of error rate and computation time, it seems suitable to say that 1,000 samples provide precise solution within reasonable computation time.

Fig. 4 illustrates the normal distribution curve for the power demand uncertainty of the test system using MCS with 1,000 samples. With larger numbers of MCS samples, the power demand histogram converged to the normal distribution curve. As shown in Fig. 4, the power demand uncertainty was very close to being distributed normally. It is confirmed once more that a sample size of 1,000 provides the optimal value of demand uncertainty fitness with reasonable computational accuracy.

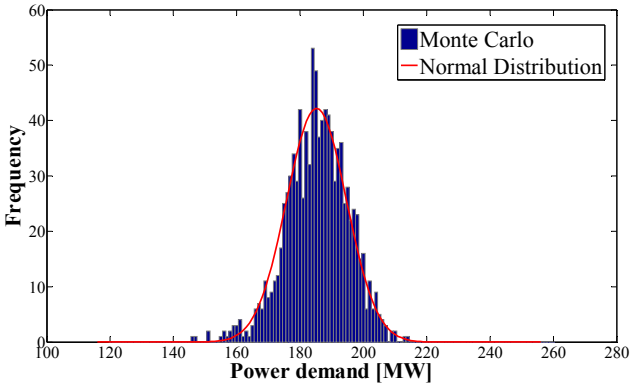

Fig. 4. Power demand uncertainty with a normal distribution.

Table 3. Relationship between the MCS sample size and performance

No. of samples	Mean value of OC [$]	Standard deviation of OC [$]	ε_σ [%]	Computation time [s]
500	607.84	3.03	1.2	56.3
1,000	608.77	1.75	0.28	118.6
3,000	608.76	1.43	0.23	352.1
5,000	608.05	1.1	0.19	594.4
10,000	608.16	1.08	0.18	1191.2

5.2. Correlated wind speed

Each Vestas V100 wind turbine had a rated power of 1.8 MW at 11 m/s, a cut-in wind speed of 3 m/s, and a cut-out wind speed of 20 m/s.

Table 4 shows the mean, standard deviation, Weibull parameters, and correlation coefficient for wind speed at the two wind farms. The mean values for the two locations were 3.32 and 3.37 m/s. Using the MATLAB *wblrnd*() function, we produced uncorrelated random variables with the two Weibull parameters for each location,

$$z = (z_1, z_2)^{\mathrm{T}} \tag{26}$$

$$\mu_z = (3.68, 3.29)^{\mathrm{T}} \tag{27}$$

$$\Omega_z = \begin{pmatrix} 1.0 & 0.07 \\ 0.07 & 1.0 \end{pmatrix} \tag{28}$$

Table 4. Results for the correlated Weibull distributions.

	Bus 8 (WF1)	Bus 21 (WF2)
Mean value μ	3.32	3.37
Standard deviation σ	1.89	1.77
Scale parameter c	3.74	3.78
Shape parameter k	1.83	1.94
Correlation coefficient	$\rho = \begin{bmatrix} 1.0 & 0.51 \\ 0.51 & 1.0 \end{bmatrix}$	

The correlated Weibull random variables $\boldsymbol{y}$ can be solved as shown in Eq. (10).

$$\begin{pmatrix} y_1 \\ y_2 \end{pmatrix} = \begin{pmatrix} 1 & 0 \\ 0.51 & 0.86 \end{pmatrix} \begin{pmatrix} z_1 - 3.68 \\ z_2 - 3.29 \end{pmatrix} + \begin{pmatrix} 3.32 \\ 3.37 \end{pmatrix} \quad (29)$$

To confirm that the correlated wind speeds V generated by Weibull random variables $\boldsymbol{y}$ actually follow the Weibull distribution, we checked them by comparison with the normal distribution model. Fig. 5 and Fig. 6 show the probability plot for Weibull and normal distributions of $\boldsymbol{y_1}$ and $\boldsymbol{y_2}$, respectively. These figures have a reference line that passes through the lower and upper quartiles of $\boldsymbol{y_1}$ and $\boldsymbol{y_2}$ (correlated Weibull random variables) to help determine whether the generated wind speeds follow the distribution. The results showed that $\boldsymbol{y_1}$ and $\boldsymbol{y_2}$ followed a Weibull distribution rather than a normal distribution.

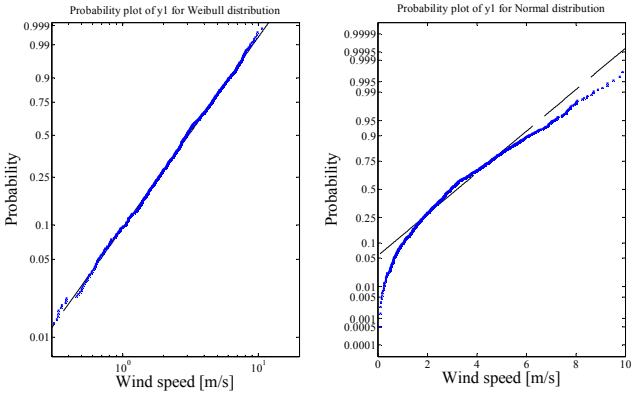

Fig. 5. Probability plot of $\boldsymbol{y_1}$ for Weibull and normal distributions.

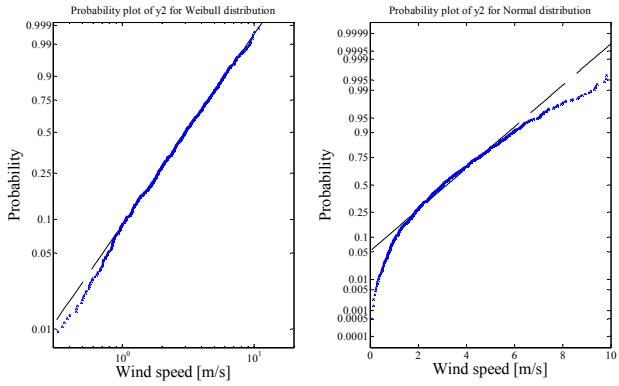

Fig. 6. Probability plot of $\boldsymbol{y_2}$ for Weibull and normal distributions.

5.3. Base case solutions

Table 5 shows the optimal solutions of P-SCOPF. The total expected operating costs were \$577.46 and \$612.84 with and without wind power, respectively. The corresponding optimal solutions consider the power demand uncertainty in both cases. A mean system demand of 189.2 MW must be covered by thermal plants and/or wind turbines.Fig. 7 and Fig. 8 represent the total expected operating cost with and without wind power, respectively. The line on each graph indicates the overall cost trend. The total expected operating cost was nearly \$36 (6%) less when wind power covered some part of the demand. Note that in these figures, the total expected operating cost with wind power integration was distributed over a wider range of the cost axis and that wind power increased the uncertainty of the total expected operating cost. Furthermore, the uncertainty in the power system due to the variability and intermittency of wind power was greater than that of the power demand.

Table 5. Optimal solutions of P-SCOPF.

		With only consideration of the load variations	With consideration of wind and load variations
Unit [MW]	G1	40.82	40.54
	G2	35.82	43.6
	G3	26.70	24.9
	G4	42.60	37.7
	G5	20.60	18.37
	G6	25.77	21.67
Total generation of thermal units [MW]		192.31	186.77
Loss [MW]		3.11	3.1
Wind Power [MW]		0	5.53
Total Cost [\$]		612.84	577.46
CO2 emission [ton]		0.272	0.256

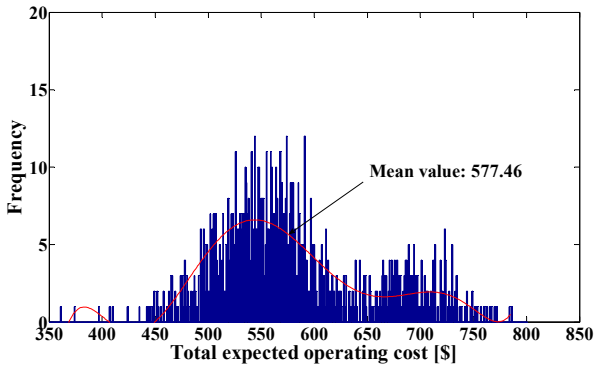

Fig. 7. Total expected operating cost with wind power.

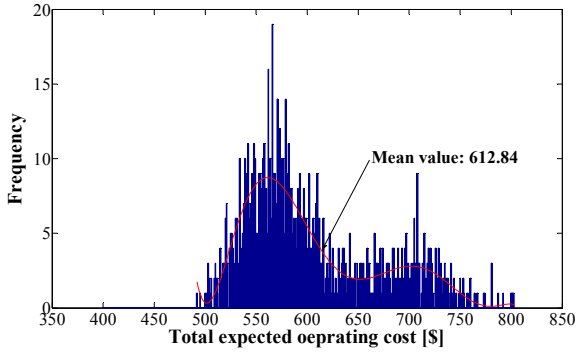

Fig. 8. Total expected operating cost without wind power.

Although wind power accounted for approximately 20% of the entire system capacity, it accounted for only 5.53 MW (2.9%) of the system generation. The capacity factor, which is the ratio of the actual output of a plant to its potential output if it had produced at maximum capacity, is generally calculated over some specific period of time. When an index was introduced to represent the efficiency of the wind power in the test system, the capacity factor was nearly 7.5% (5.53 / 72 MW).

Fig. 9 and Fig. 10 describe the power transfer through lines 6-8 and 22-21, which were connected to the wind farm buses. We concentrated on these two lines, which were directly influenced by the wind power generation. These figures showed that the power injected through the lines closest to the wind farm buses decreased because the generated wind power covered the demand of its own bus.

Table 6 and Fig. 11 and show the total expected operating cost and CO_2 emissions as a function of the installed wind power capacity. The total expected operating cost and CO_2 emissions decreased as the installed wind power capacity increased. When wind power was approximately 20% of the total generation capacity, the total expected operating cost and CO_2 emissions decreased by roughly \$35.4 (6%) and 0.016 tons (5.7%), respectively. Wind power generation is directly proportional to installed wind power. On the other hand, reduction in total expected operating cost and CO_2 emissions decreases as the installed wind power increases. The most expensive and most polluting thermal units reduce their power output as wind power is integrated into traditional power systems. This implies that wind power is the most cost effective and environmentally friendly in the early integration stage.

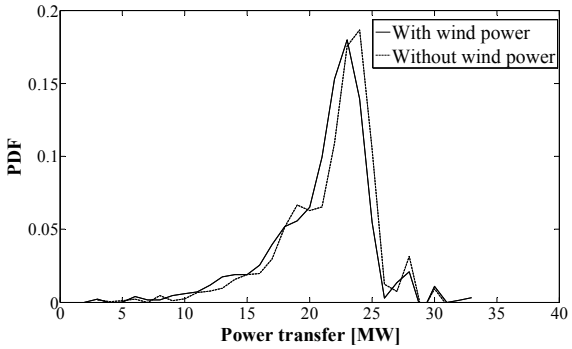

Fig. 9. Power transfer of line 6-8.

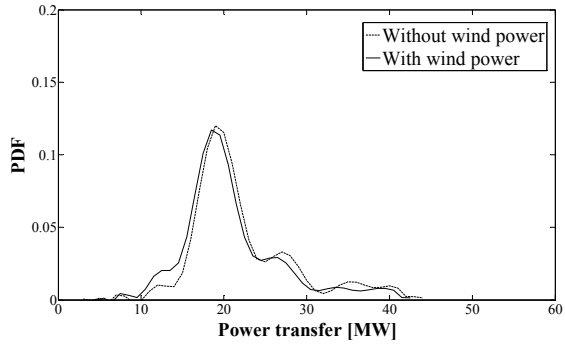

Fig. 10. Power transfer of line 22-21.

Transmission network losses are seldom affected by wind power integration. Since we treated wind power like a negative demand on the bus, wind power integration had little effect on large changes in power transfer except on the buses adjacent to wind farms. The number of MCS samples significantly influenced the trade-off between solution accuracy and computation time. Using 1,000 MCS samples was sufficient to produce good results within an acceptable computation time of 137.3 s.

5.4. Contingency case solutions

This section describes how the P-SCOPF solution is obtained when the test system is subjected to different types of transmission line contingency. Contingency analysis could be performed over a set of plausible contingencies. In this study, the following critical contingencies were selected based on the relative mean values of the real power performance index (PI) [10]:

Table 7 summarizes the total expected operating costs

Table 6. Total expected operating cost and CO_2 emission versus the installed wind power.

Installed wind power [MW]	Wind power generation [MWh]	Total expected operating cost [\$]	CO2 emission [ton]
0	0	612.84	0.272
18 (10 wind turbines)	1.32	597.4 (-15.44)	0.265 (-0.07)
36 (20 wind turbines)	2.62	589.3 (-8.1)	0.26 (-0.05)
54 (30 wind turbines)	3.95	582.2 (-7.1)	0.258 (-0.02)
72 (40 wind turbines)	5.53	577.4 (-4.7)	0.256 (-0.02)

(a) N-1: outage of line 6-8
(b) N-2: outage of lines 6-8 or 8-28
(c) N-3: outage of lines 6-8, 8-28, or 28-27
(d) N-4: outage of lines 6-8, 8-28, 28-27, or 6-7
(e) N-5: outage of lines 6–8, 8–28, 28–27, 6–7, or 27–30

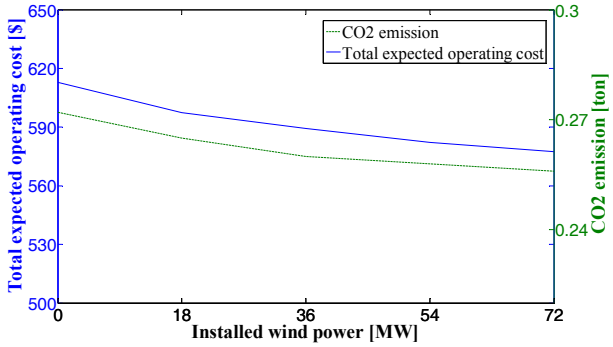

Fig. 11. Total expected operating cost and CO_2 emissions as functions of the installed wind power.

Table 7. Total expected operating costs under contingency conditions.

Contingency Condition	Total Expected Operating Cost [$]
No contingency	577.46
(a)	580.1
(b)	583.5
(c)	643
(d)	719.1
(e)	725.2

for the various contingency cases. Note that the total expected operating costs in the contingency cases increased due to the dispatch of more-expensive units to cover additional possible contingencies. That is, the system operator tried to relieve the congestion management infeasibility and maintain system security during the contingency-based rescheduling operation.

6. Conclusion

This paper proposes a novel probabilistic approach for investigating the impacts of wind power integration. A major contribution of this paper is the development of the P-SCOPF algorithm, which considers the system security problem. The two uncertainties of demand and wind speed were modeled using the normal distribution and Weibull distribution, respectively. The method used correlated wind speeds to obtain the aggregate wind generation from all wind farms that contribute to solving the P-SCOPF. MCS was used to choose input variables of demand and wind speeds from their PDFs. Test results on a modified IEEE 30-bus system demonstrated the feasibility of the proposed approach to solving the P-SCOPF problem. Comprehensive numerical results confirmed that the demand and correlated wind speeds closely followed normal and Weibull distributions, respectively. The introduction of wind speed correlation also enabled more realistic and accurate evaluations of the distribution function of power transfers through the lines. Due to the probabilistic nature of the uncertainties, all outcomes including total expected operating cost and power transfer resulted in PDF forms. The mean value of total expected operating cost as well as CO_2 emissions decreased as the installed wind power increased. Furthermore the power injected into the bus connected to the wind farm decreased because of the wind power generation. When contingency constraints are imposed, the operating cost is higher than in the base case, as the system would be operated in a more conservative manner. This approach provides a trade-off among economics, uncertainty, security, and good computational accuracy. This produces useful information for independent system operators under conditions of vulnerability in a deregulated power industry.

Acknowledgements

This work was supported by the National Research Foundation of Korea (NRF) grant funded by the Korea government (MEST) (2012-0009145).

Nomenclature

i	Index for bus
n	Index for wind farm
m	Index for wind turbine
N_G	Number of units
$N_{WT,n}$	Number of wind turbines in n-th wind farm
N_c	Number of contingencies
N_{WF}	Number of wind farms
N_B	Number of buses
a_i, b_i, c_i	Coefficients of the quadratic production cost function of unit i
$\alpha_i, \beta_i, \gamma_i, \zeta_i, \lambda_i$	Coefficients of the CO_2 emission function of unit i
$f(\cdot)$	Probabilistic distribution function
V	Random variable of wind speed
v	Wind speed element
v_{in}	Cut-in speed
v_r	Wind turbine rated speed
v_{out}	Cut-out speed
P_i	Power output of thermal generating unit i
P_D	Power demand
P_L	Transmission network losses of system
$P_W(v)_{n,m}$	Generated wind power from m-th wind turbine of n-th wind farm
μ_{PD}	Mean value of power demand
σ_{PD}	Standard deviation of power demand
μ_V	Mean value of wind speed
σ_V	Standard deviation of wind speed
c	Scale factor of Weibull distribution
k	Shape factor of Weibull distribution
$\boldsymbol{y}$	Correlated Weibull random variable vectors
L	Cholesky decomposition matrix
Γ	Legendre's gamma function
$A_{l,i}$	Sensitivity of the flow on line l to the generation at bus i
$P_{\Phi,i}$	Equivalent power injection from phase shifter to unit i
$P_{D,i}$	Power demand at bus i

References

[1] J. Kabouris, F.D. Kanellos, "Impacts of Large Scale Wind Penetration on Energy Supply Industry", *Energies*, Vol. 2, No. 4, pp. 1031-1041, Nov 2009.

[2] A. Franco, P. Salza, "Strategies for optimal penetration of intermittent renewables in complex energy

systems based on techno-operational objectives", *Renewable Energy*, Vol. 36, No. 2, pp. 743-753, Aug 2010.

[3] B. Borkowska, "Probabilistic load flow". *IEEE Trans Power Appa Syst*, Vol. 93, No. 3, pp. 752-755, May 1974.

[4] C.L. Su, "Probabilistic load flow computation using point estimate method", *IEEE Trans Power Syst*, Vol. 20, No. 4, pp. 1843-1851, Nov 2005.

[5] G. Verbic, C.A. Canizares, "Probabilistic optimal power flow in electricity markets based on a two-point estimate method. *IEEE Trans Power Sys*, Vol. 21, No. 4, pp. 1883-1893, Nov 2006.

[6] H. Ahmadi, H. Ghasemi, "Probabilistic optimal power flow incorporating wind power using point estimate methods. *10th Int Conf Envir Elec Eng* May 2011.

[7] A. Schellenberg, W. Rosehart, J. Aguado, "Cumulant-based probabilistic optimal power with gaussian and gamma distribution". *IEEE Trans Power Syst*, Vol. 20, No. 2, pp. 773-781, May 2005.

[8] X. Li, Y. Li, Y, S. Zhang, "Analysis of probabilistic optimal power flow taking account of the variation of load power", *IEEE Trans Power Syst*, Vol. 23, No. 3, pp. 992-999, Aug 2008.

[9] J. Wang, M. Shahidehpour, Z. Li, "Security-constrained unit commitment with volatile wind power generation", *IEEE Trans Power Syst*, Vol. 23, No. 3, pp. 1319-1327, Aug 2008.

[10] J. K. Lyu, M. K. Kim, Y. T. Yoon, J. K. Park, "A new approach to security-constrained generation scheduleing of large-scale power systems with a piecewise linear ramping model", *Int J Electric Power Energy Syst*, Vol. 34, No. 1, pp. 121-131, Jan 2012.

[11] F. Capitanescu, J.L.M. Ramos, P. Panciatici, D. Kirschen, A.M. Marcolini, L. Platbrood, L. Wehenkel, "State-of-the-are, challenges, and future trends in security constrained optimal power flow. *Elect Power Syst Res*, Vol. 81, No. 8, pp. 1731-1741, Aug 2011.

[12] P. Somasundaram, K. Kuppusamy, "Application of evolutionary programming to security constrained economic dispatch", *Int J Electric Power Energy Syst*, Vol. 27, No. 5-6, pp. 343-351, July 2005.

[13] R. Goic, J. Krstulovic, D. Jakus, "Simulation of aggregate wind farm short-term production variations", *Renewable Energy*, Vol. 35, No. 11, pp. 2602-2609, Nov 2010.

[14] S. H. Isidoro, E. E. Guillermo, A. O. Manuel, "Wind farm electrical power production model for load flow analysis. *Renewable Energy*, Vol. 36, No. 3, pp. 1008-1013, Mar 2011.

[15] A. Feijoo, D. Villanueva, J. L. Pazos, R. Sobolewski, "Simulation of correlated wind speeds: a review", *Renewable and Sustainable Energy Reviews*, Vol. 15, No. 6, pp. 2826-2832, Aug 2011.

[16] D. Villanueva, A. Feijoo, J.L. Pazos, "Probabilistic load flow considering correlation between generation, loads and wind power", *Smart grid and Renewable Energy*, Vol. 2, No.1, pp. 12-20, Feb 2011.

[17] F. Freris, D. Infield, "Renewable energy in power systems. New York; John Wiley and Sons: 2008.

[18] P. Ramirez, J. A. Carta, "Influence of the data sampling interval in the estimation of the parameters of the Weibull wind speed probability density distribution: a case study. *Energy Conv Mana*, Vol. 46, Nol. 15-16, pp. 2419-2438, Sep 2005.

[19] S.A. Akdag, A. Dinler, "A new method to estimate Weibull parameters for wind energy applications", *Energy Conv Mana*, Vol. 50, No. 7, pp. 1761-1766, July 2009.

[20] M.A. Abido, "Multiobjective evolutionary algorithms for electric power dispatch problem", *IEEE Trans Evol Comp*, Vol. 10, No. 3, pp. 315-329, June 2006.

[21] H. Wei, H. Sasaki, J. Kubokawa, R. Yokoyama, "An interior point nonlinear programming for optimal power flow problems with a novel data structure. Power Systems, *IEEE Trans Power Syst*, Vol. 13, No. 3, pp. 870-877, Aug 1998.

[22] F. Capitanescu, M. Glavic, D. Ernst, L. Wehenkel, "Interior-point based algorithms for the solution of optimal power flow problems. *Elect Power Syst Res*, Vol. 77, No. 5-6, pp. 508-517, April 2007.

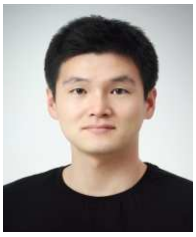

Jae-kun Lyu was born in Korea, on 1982. He received the B.S. degree in electrical engineering from Shinshu University, Nagano, Japan in 2006. Currently he is working on the Integrated Master's and Doctor's Course in the Department of Electrical Engineering at Seoul National University. His research field of interest includes power system operation and reliability, renewable energy integration.

Jae-Haeng Heo was born in Korea in 1978. He received his B.S. degree in Electrical Engineering from Dankook University, Seoul, Korea in 2005 and his M.S. degree in Electrical Engineering from Seoul National University, Seoul, Korea. He is currently working on his Ph.D. course in the Department of Electrical Engineering at Seoul National University. His research field of interest includes power system reliability.

Mun-Kyeom Kim was born in Korea, on 1976. He received B.S. degree in Electrical Engineering from Korea University, Seoul, Korea in 2004 and M.S. and Ph.D. degrees in Electrical Engineering from Seoul National University, Seoul, Korea in 2006 and 2010, respectively. He worked as a post-doc in the institute of information technology in the department of electrical engineering at Seoul National University. He is currently a assistant professor in the Department of Electrical Engineering, Dong-A University, Busan, Korea in 2011. His research interests include the electric power network economics, power system reliability, and the real-time market design in smart grid

Jong Keun Park was born in Republic of Korea in 1952. He received B.S. degree in electrical engineering from Seoul National University, Korea in 1973 and his M.S. and Ph.D. degrees in electrical engineering from The University of Tokyo, Japan in 1979 and 1982, respectively. He worked as a Researcher at the Toshiba Heavy Apparatus Laboratory in 1982. He was a Visiting Professor with the Technology and Policy Program and Laboratory for Electromagnetic and Electronic Systems, Massachusetts Institute of Technology, Cambridge, in 1992. He is currently a Professor in the School of Electrical Engineering, Seoul National University. He is a senior member of the Institute of Electrical and Electronics Engineers (IEEE) and a fellow of the Institution of Electrical Engineers (IEE) and a member of the National Academy of Engineering of Korea and the Korean representative of the study committee SC5 “Electricity Markets and Regulation” in CIGRE. Also he was a President of Korean Institute of Electrical Engineers (KIEE) in 2010.